

Relation of reflectance intensity and chemical contents of oil palm fresh fruit bunches using multispectral imaging

Nisa Arpyanti, Minarni Shiddiq*, Rahmondia Nanda Setiadi, Fisal Rabin,
Ihsan Okta Harmailil, Vicky Vernando Dasta

Department of Physics, Universitas Riau, Pekanbaru 28293, Indonesia

*Corresponding author: minarni.shiddiq@lecturer.unri.ac.id

ABSTRACT

Multispectral imaging has been widely used for the classification of fruits and vegetables. This technique offers both spectral and spatial resolution, enabling the evaluation of fruit quality based on its chemical properties. This study aims to analyze the relationship between reflectance intensity obtained from multispectral imaging and the chemical composition of oil palm fresh fruit bunches (FFBs), specifically oil content and free fatty acid (FFA) levels, measured using the Soxhlet extraction method. The multispectral imaging system consists of a monochrome camera and an LED light source with eight wavelengths ranging from 680 nm to 900 nm. FFB images were processed using Python scripts to extract reflectance intensity. The Python scripts were also used to analyze the correlation between reflectance intensity and both oil content and FFA levels. A total of 15 unripe and 15 ripe FFB samples were used. Correlation analysis was focused on the 780 nm wavelength due to its high reflectance intensity. The results showed that the correlation coefficient between reflectance intensity and oil content was $r = -0.39$ for unripe fruits and $r = 0.29$ for ripe fruits, while the combined data yielded a strong correlation of $r = 0.92$. For FFA, the correlation was $r = -0.41$ for unripe fruits, $r = -0.34$ for ripe fruits, and $r = 0.72$ for the combined dataset. These findings demonstrate that multispectral imaging is a promising non-destructive method for classifying the ripeness of oil palm FFBs based on oil content and FFA levels.

Keywords: Free fatty acid; multispectral imaging; oil content; oil palm fresh fruit bunch; ripeness

Received 26-05-2025 | Revised 10-06-2025 | Accepted 17-06-2025 | Published 31-07-2025

INTRODUCTION

Multispectral imaging is one of the imaging techniques widely used in the agricultural sector to evaluate fruits and vegetables. This method combines spectroscopy with traditional imaging techniques, resulting in images that possess both spectral and spatial resolution. Multispectral imaging enables the evaluation of internal characteristics of fruits across a broad range of wavelengths, including ultraviolet (UV), visible, and infrared regions. In contrast, traditional imaging is limited to a narrower spectral range, typically confined to the three visible bands: Red, Green, and Blue (RGB). The application of multispectral imaging in agriculture is extensive and includes various uses for crops, fruits, and vegetables. These applications include monitoring seed health and quality [1], detecting citrus greening disease

[2], monitoring olive tree growth [3], and evaluating the ripeness of oil palm fresh fruit bunches (FFB) [4].

The prediction of chemical composition using multispectral and hyperspectral imaging has been widely applied as a non-destructive method in the agricultural sector. This approach relies on spectral information generated from the interaction between light and the sample across various wavelengths, enabling the identification and quantification of specific chemical compounds such as moisture, sugar, oil, and free fatty acids without damaging the sample. This method, commonly referred to as chemometrics, serves as an alternative to conventional techniques such as Soxhlet extraction, which are time-consuming and require skilled personnel. Several applications of multispectral and hyperspectral imaging for chemical content prediction include the

estimation of moisture, dry matter, and firmness in date cultivars [5], as well as oil content prediction in maize seeds [6].

Currently, LED (light-emitting diode)-based multispectral imaging systems are widely used due to their cost-effectiveness compared to systems utilizing filter wheels. The primary components of this system include an LED light source and a monochrome camera equipped with a lens. The LED light source consists of an array of LEDs with different wavelengths, which can be activated sequentially. This LED array replaces halogen lamps, whose light is typically filtered using color filters mounted on a filter wheel. The LEDs used in this configuration generally have narrow bandwidths but offer fast response times and allow rapid switching between wavelengths via current control. However, the spectral resolution tends to be lower due to the limited availability of LEDs at certain required wavelengths [7]. One of the advantages of using a monochrome camera is its broader sensitivity range, extending from ultraviolet (UV) to infrared (IR) regions [8].

Image processing is a critical step in multispectral imaging for evaluating fruits and vegetables. Reflectance intensity is the key parameter extracted from multispectral images. The image processing workflow begins with image calibration to correct for uneven lighting and sensor response. Calibration is performed by subtracting the object image with the white reference and black reference images. Following calibration, image segmentation is conducted to isolate the primary object from the background. After segmentation, the reflectance intensity at each wavelength is determined [9]. This reflectance intensity value represents the proportion of light reflected from the surface of the object at a specific wavelength, which can then be correlated with chemical parameters such as oil content, moisture, or free fatty acid levels.

Crude Palm Oil (CPO) is one of Indonesia's largest export commodities. The quality of CPO is significantly influenced by various factors, one of which is the quality of Fresh Fruit

Bunches (FFB). A key determinant of FFB quality is the ripeness level, which is closely related to its oil content and free fatty acid (FFA) levels. The sorting and grading process of FFB in palm oil mills (POMs) is essential to ensure high-quality raw materials. However, this process is still predominantly carried out manually. Manual sorting is based on external attributes of the fruit, such as the number of loose fruits (brondolan) and changes in fruit color. This manual approach has several drawbacks, including subjectivity and operator fatigue during prolonged working periods [10]. Grading involves determining FFB quality based on internal characteristics such as oil and moisture content. This process requires skilled personnel, expensive equipment, and a significant amount of time [11]. Currently, non-destructive methods based on imaging and machine learning are being developed to enable faster and real-time sorting and grading of FFB [12].

This study aims to analyze the relationship between reflectance intensity and the chemical composition of Fresh Fruit Bunches (FFB), specifically oil content and free fatty acid (FFA) levels. The correlation between these variables is represented by the correlation coefficient. Reflectance intensity is derived from images obtained using an LED-based multispectral imaging system. Oil content and FFA levels are measured using the Soxhlet extraction method. The imaging system employs a monochrome camera and an array of LEDs with eight different wavelengths ranging from 680 to 900 nm. Python programming is utilized for image acquisition, processing, and the analysis of the correlation between reflectance intensity and chemical composition.

RESEARCH METHODS

This study utilizes an LED-based multispectral imaging system to investigate the relationship between the reflectance intensity of oil palm Fresh Fruit Bunches (FFB) and their chemical composition at two ripeness levels: unripe and ripe. The research consists of three

main stages: image acquisition, multispectral image processing, and the measurement of oil content and free fatty acid (FFA) levels. Each of these stages is interconnected and is illustrated in the flowchart presented in Figure 1.

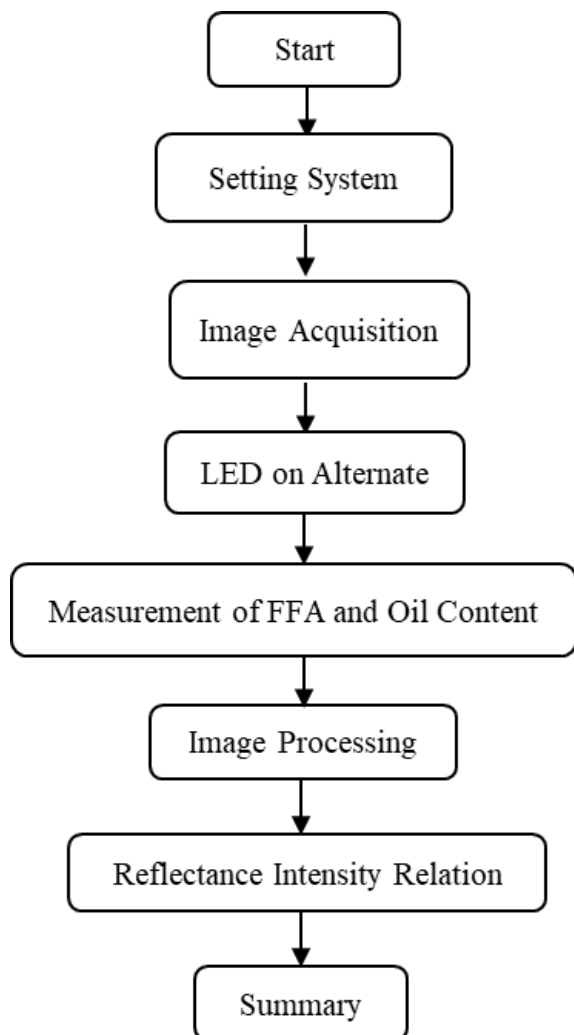


Figure 1. Research flowchart.

Image Acquisition

Figure 2 illustrates the schematic of the LED-based multispectral imaging system, which consists of a donut-shaped LED ring array with a monochrome camera positioned at the center. The LED array comprises eight different wavelengths: 680 nm, 700 nm, 750 nm, 780 nm, 800 nm, 850 nm, 880 nm, and 900 nm [13]. This LED unit replaces the conventional white light source combined with color filters, as the LEDs can be turned on and

off individually using a current supply that enables rapid switching. In this study, each LED of a specific wavelength is activated sequentially, and the camera captures an image for each illumination. As a result, for every FFB sample, eight images are obtained, each corresponding to a different wavelength.

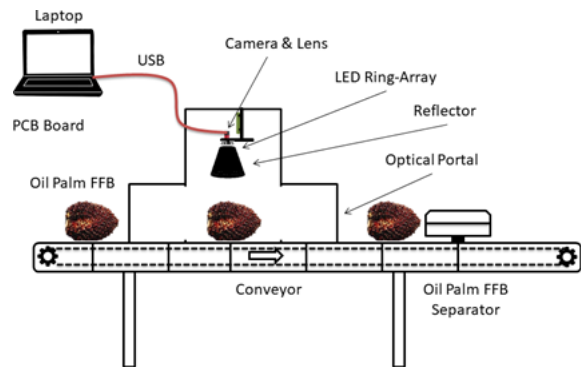


Figure 2. Multispectral imaging system.



Figure 3. Oil palm fresh fruit bunches.

Figure 3 shows the FFB samples used in this study. The samples are categorized into two classes: unripe and ripe. Unripe FFB are characterized by the absence of loose fruits (brondolan) and have a dark purple to black coloration. In contrast, ripe FFB exhibit some degree of fruit detachment, with the bunch appearing reddish-yellow to orange in color. A total of 30 FFB samples were used in the study, consisting of 15 unripe and 15 ripe bunches.

Image Processing

The image processing system is divided into two components: hardware and software. The hardware consists of a laptop and USB cables that connect the camera and LED array to the laptop, allowing both to be directly controlled via an application on the computer. The laptop serves to provide commands to the camera and LEDs during the image acquisition process. On the other hand, the software component utilizes a Python-based program to process the image data captured by the camera. Image acquisition was carried out on 30 samples of oil palm Fresh Fruit Bunches (FFB), with two images taken from the front and back sides of each FFB, resulting in a total of 16 images per sample.

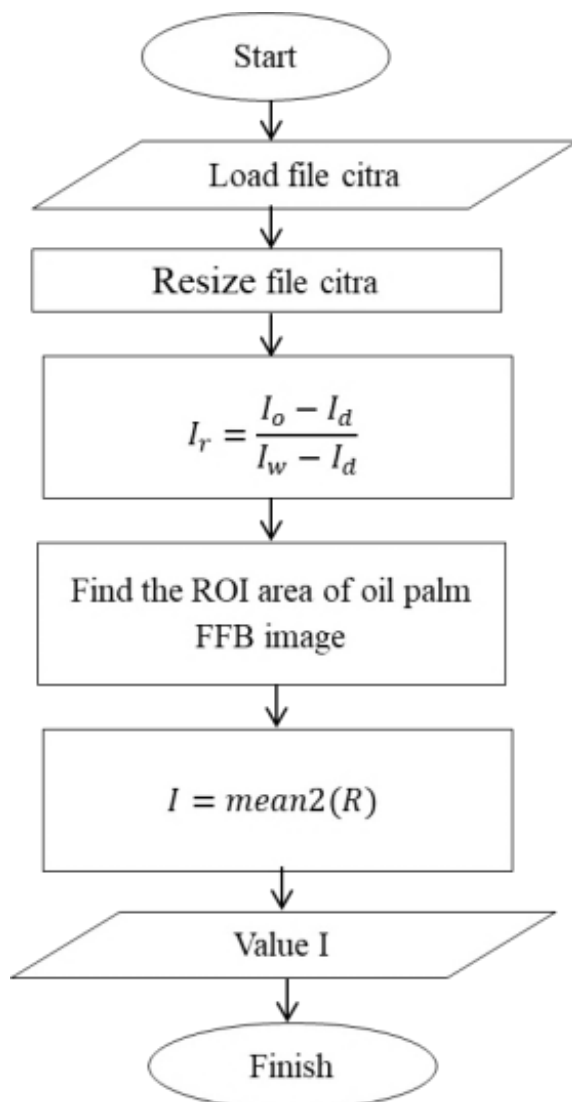


Figure 4. Oil palm fresh fruit bunches.

Multispectral image processing was performed using Python scripts following the data acquisition stage. Three types of images were processed: the sample image, the white reference, and the black reference. The white reference was used as a standard for maximum reflectance intensity, while the black reference served to eliminate the effect of dark current from the detector. These three images were then corrected and converted into an intensity matrix, which was ready for further analysis. Figure 4 was used to determine the average reflectance intensity (I_r), which was utilized in this study [14].

Chemical Content Measurement

Oil content and free fatty acid (FFA) measurements were carried out using a destructive method based on Soxhlet extraction. Since oil and FFA levels are highly sensitive to time, the measurements were performed immediately after image acquisition to maintain accuracy. The oil content measurement process began with collecting fruitlets from various parts of the Fresh Fruit Bunch (FFB), which were then peeled, ground, dried in an oven, and extracted using n-hexane solvent. The extract was then processed through Soxhlet extraction, followed by distillation, and finally weighed to obtain the oil mass. Meanwhile, FFA measurement was performed by extracting palm fiber using neutral alcohol, adding phenolphthalein indicator, and titrating the solution with a sodium hydroxide (NaOH) solution. All procedures were conducted immediately after sampling to ensure accurate and representative results for determining the ripeness level of the FFB [14].

RESULTS AND DISCUSSION

Reflectance Intensities

Multispectral image analysis was conducted on 30 Fresh Fruit Bunches (FFB) with two ripeness levels. The multispectral imaging system captured images using a monochrome

camera and an LED light source. The recorded images were then processed by applying white and black reference corrections [14]. Unripe fruits exhibit a dark purplish skin color, whereas ripe fruits display a reddish-orange hue. Figure 5 shows the average reflectance intensity of 15 unripe FFBs (blue) and 15 ripe FFBs (red) across each wavelength.

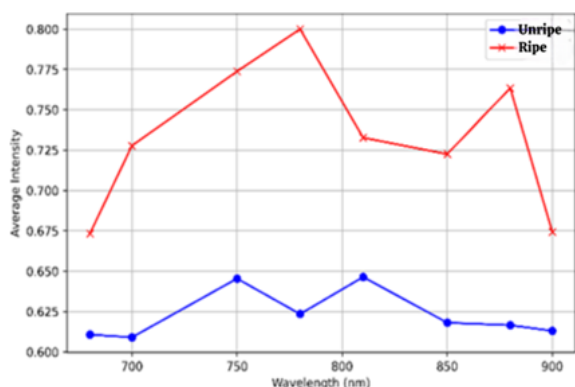


Figure 5. Average reflectance intensity at each LED wavelength for the two ripeness levels.

Figure 5 illustrates the average reflectance intensity at each LED wavelength used. Each data point represents the mean intensity derived from images of 15 FFB samples for each wavelength. Based on Figure 5, the reflectance intensity for the unripe category tends to increase at wavelengths of 750 nm and 810 nm. In contrast, the ripe category shows an increase at 750 nm, 780 nm, and 880 nm. However, both categories exhibit a decrease in reflectance intensity at wavelengths of 680 nm and 700 nm, indicating that the images at these wavelengths appear fainter compared to the others.

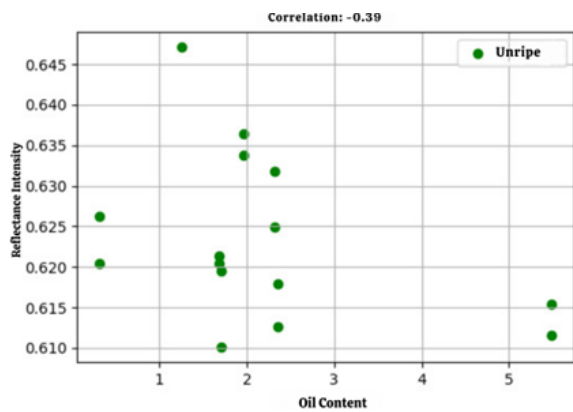
The interaction of infrared light with the chemical content of oil palm Fresh Fruit Bunches (FFB) influences the reflectance curve observed in Figure 5. Generally, as the fruit ripens, the red coloration produced by carotenoid compounds in oil palm increases. This indicates that the surface of ripe fruit reflects more light than that of unripe fruit. The wavelength range of 700 – 900 nm lies within the infrared spectrum, where electromagnetic waves interact at the molecular level, particularly with compounds such as anthocyanins. The anthocyanin content in ripe

oil palm fruit is typically higher than in unripe fruit [15]. In the wavelength range of 680–750 nm, the reflectance intensity for both ripe and unripe samples remains relatively low. This phenomenon is likely due to the high absorption of light by chlorophyll pigments or other surface pigments found on oil palm fruit, especially in unripe samples [16].

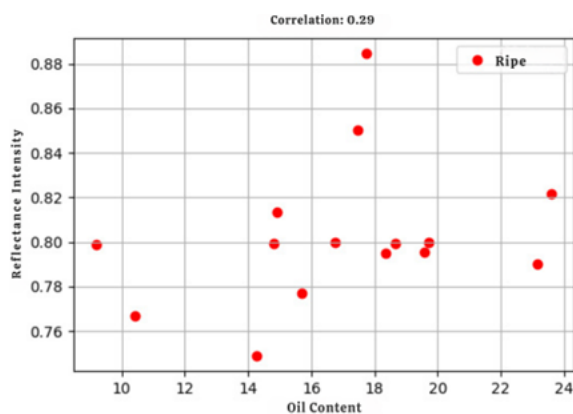
Correlation Between Reflectance Intensity and Oil Content in Oil Palm Fruit

Based on the three graphs presented in Figure 6, the relationship between reflectance intensity and oil content is analyzed for two ripeness levels unripe and ripe as well as for the combined dataset. Figure 6 (a), which displays data exclusively for unripe fruit, reveals a negative correlation between reflectance and oil content, with a correlation coefficient of $r = -0.39$. This suggests that, in unripe oil palm fruit, an increase in oil content corresponds to a decrease in reflectance intensity. The internal structure of unripe fruit typically exhibits higher moisture content and denser tissue, which leads to greater absorption and multiple scattering of incident light. These optical properties result in a lower proportion of light being reflected back to the sensor [16]. From an optical standpoint, wet and complex biological tissues tend to absorb more light and produce diffuse scattering, thereby reducing coherence and directionality of reflected light [17].

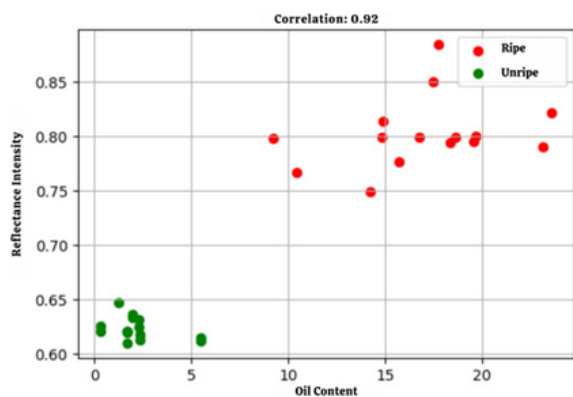
Figure 6 (b) illustrates the relationship observed in ripe fruit, showing a positive correlation with a coefficient of $r = 0.29$. This suggests that as oil content increases, reflectance intensity also tends to increase, although the relationship is not statistically significant. The weakness of this correlation may be attributed to surface variability in ripe fruits and the non-uniform internal distribution of oil [18]. Reflectance in ripe fruit is strongly influenced by the complex interaction between light scattering and the spatial distribution of chemical compounds (such as oil and pigments), which may not follow a linear pattern.



(a)



(b)

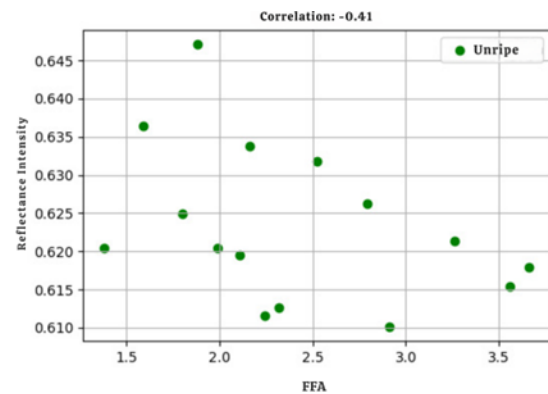


(c)

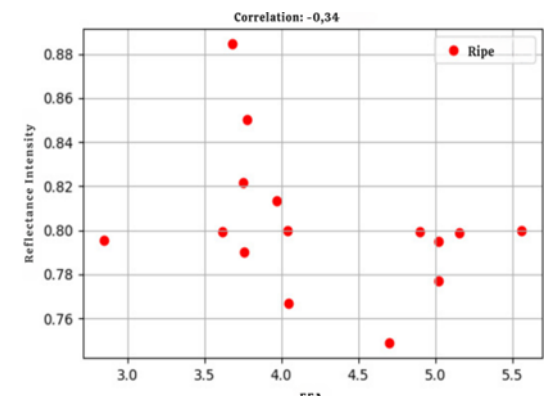
Figure 6. Correlation between relative reflectance intensity at 780 nm and oil content in oil palm fresh fruit bunch.

Figure 6 (c) presents the correlation between reflectance intensity and oil content based on the combined dataset of both unripe and ripe fruits. The result reveals a very strong positive correlation with a coefficient of $r = 0.92$, indicating that reflectance increases consistently with rising oil content. This phenomenon can be explained from a photonic perspective: ripe fruits with higher oil content

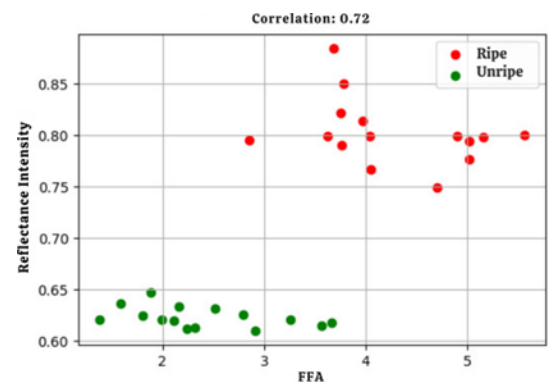
and lower moisture levels compared to unripe ones tend to exhibit a higher internal refractive index and more organized light scattering behavior [19]. These optical characteristics lead to greater reflectance, suggesting that the accumulation of lipophilic compounds such as oil within the fruit tissue enhances reflectance at specific wavelengths.



(a)



(b)



(c)

Figure 7. Correlation between relative reflectance intensity at 780 nm and free fatty acid (FFA) content.

Figure 7 represents the correlation between reflectance intensity and free fatty acid (FFA) content in oil palm fruit at different ripeness levels: unripe, ripe, and the combined dataset. Reflectance intensity refers to the fraction of light energy that is reflected back after electromagnetic waves—typically in the visible or near-infrared spectrum—interact with the surface of biological materials, in this case, the surface of oil palm fruit. Reflectance is strongly influenced by the optical properties of the fruit tissue, including the refractive index, absorption coefficient, cellular structure, and internal chemical composition.

In Figure 7 (a), which presents the data for unripe fruit, a negative correlation of $r = -0.41$ is observed between reflectance intensity and free fatty acid (FFA) content. This indicates that as FFA levels increase, reflectance values tend to decrease. This decline is likely due to the high moisture content and dense cellular structure of unripe fruit, which result in increased absorption coefficients and internal light scattering. The presence of hydrophilic compounds and tissue density may lead to a reduction in spectral reflectance [16].

Figure 7 (b) illustrates the relationship for ripe fruit, showing a weaker negative correlation of $r = -0.34$ between reflectance and FFA content. Although both unripe and ripe fruits exhibit a decrease in reflectance with rising FFA levels, the optical interaction in ripe fruit is more complex. This is due to tissue softening and elevated levels of oil and phenolic compounds, which affect light interaction within the biological matrix [19]. Phenolic compounds and lipid degradation may alter spectral absorption properties by modifying the refractive index and influencing light absorption behavior in plant tissue.

Figure 7 (c) displays the combined data from both unripe and ripe fruit, where the correlation between reflectance intensity and FFA content becomes strongly positive, with a correlation coefficient of $r = 0.72$. This inversion suggests a significant optical contrast between the two ripeness levels. Ripe fruits tend to have higher FFA levels and simultaneously exhibit greater

reflectance, likely due to increased lipid content and reduced moisture levels, which lead to lower absorption and higher light reflectivity. In tropical fruits, high oil content can produce enhanced reflectance spectra as a result of reduced absorption in the near-infrared region.

CONCLUSION

Multispectral imaging proved effective as a non-destructive method for evaluating oil palm fresh fruit bunches (FFBs). Reflectance intensity, especially at 780 nm, showed strong correlations with oil content ($r = 0.92$) and free fatty acids ($r = 0.72$) when both ripeness levels were combined. These results highlight the potential of multispectral imaging for rapid and objective grading of FFBs in palm oil mills.

ACKNOWLEDGEMENTS

The authors would like to acknowledge DRTPM, Universitas Riau Institute of Research and Community Service (LPPM) and PTPN V Indonesia for supporting this study. This study was funded by DRTPM under Research Grant with contract number of 157/E5/PG.02.00.PL/2023.

REFERENCES

1. ElMasry, G., Mandour, N., Al-Rejaie, S., Belin, E., & Rousseau, D. (2019). Recent applications of multispectral imaging in seed phenotyping and quality monitoring—An overview. *Sensors*, **19**(5).
2. Chang, A., Yeom, J., Jung, J., & Landivar, J. (2020). Comparison of canopy shape and vegetation indices of citrus trees derived from UAV multispectral images for characterization of citrus greening disease. *Remote Sensing*, **12**(24), 4122.
3. Jurado, J. M., Ortega, L., Cubillas, J. J., & Feito, F. R. (2020). Multispectral mapping on 3D models and multi-temporal monitoring for individual characterization of olive trees. *Remote Sensing*, **12**(7).

4. Shiddiq, M., Herman, H., Arief, D. S., Fitra, E., Husein, I. R., & Ningsih, S. A. (2022). Wavelength selection of multispectral imaging for oil palm fresh fruit ripeness classification. *Appl. Opt.*, **61**.
5. Ibrahim, A., Alghannam, A., Eissa, A., Firtha, F., Kaszab, T., Kovacs, Z., & Helyes, L. (2021). Preliminary study for inspecting moisture content, dry matter content, and firmness parameters of two date cultivars using an NIR hyperspectral imaging system. *Frontiers in Bioengineering and Biotechnology*, **9**.
6. Zhang, L., Wang, Y., Wei, Y., & An, D. (2022). Near-infrared hyperspectral imaging technology combined with deep convolutional generative adversarial network to predict oil content of single maize kernel. *Food Chemistry*, **370**.
7. Monsalve, M. A. T., Osorio, G., Montes, N. L., Lopez, S., Cubero, S., & Blasco, J. (2020). Characterization of a multispectral imaging system based on narrow bandwidth power LEDs. *IEEE Trans. Instrum. Meas.*, **70**, 1–11.
8. Crowther, J. (2022). Monochrome camera conversion: Effect on sensitivity for multispectral imaging (Ultraviolet, Visible, and Infrared). *Journal of Imaging*, **8**(3), 54.
9. Jia, B., Wang, W., Ni, X., Lawrence, K. C., Zhuang, H., Yoon, S. C., & Gao, Z. (2020). Essential processing methods of hyperspectral images of agricultural and food products. *Chemometrics and Intelligent Laboratory Systems*, **198**.
10. Lai, J. W., Ramli, H. R., Ismail, L. I., & Wan Hasan, W. Z. (2023). Oil palm fresh fruit bunch ripeness detection methods: A systematic review. *Agriculture*, **13**(1), 156.
11. Tantanawat, T., Srimongkol, S., Yuttawiriya, R., Haewchin, A., Sangkapes, T., & Hattha, E. (2020). Development of a method for measuring oil content in oil palm mesocarp using a single-outlet piston press: a feasibility study. *Journal of Food Measurement and Characterization*, **14**(1).
12. Mansour, M. Y. M. A., Dambul, K. D., & Choo, K. Y. (2022). Object detection algorithms for ripeness classification of oil palm fresh fruit bunch. *International Journal of Technology*, **13**(6), 1326–1335.
13. Rabin, M. F., Shiddiq, M., Setiadi, R. N., Harmailil, I. O., Ramdani, R., & Permana, D. (2024). Classification of maturity levels of oil palm fresh fruit bunches using LED-based multispectral imaging methods and principal component analysis. *Indonesian Physics Communication*, **21**(1), 91–98.
14. Husein, I. R., Ningsih, S. A., & Alfahrezi, G. (2023). Oil Content and Free Fatty Acid Prediction of Oil Palm Fresh Fruit Bunches Using Multispectral Imaging and Partial Least Square Algorithm. Proceedings of the 4th International Seminar on Science and Technology (ISST 2022), **7**, 143.
15. Sinambela, R., Mandang, T., Subrata, I., & Hermawan, W. (2020). A ripeness study of oil palm fresh fruit at the bunch different positions. *Jurnal Keteknik Pertanian*, **8**.
16. Ningsih, S. A., Shiddiq, M., Arief, D. S., & Husein, I. R. (2020). Penggunaan pencitraan multispektral pada panjang gelombang 520 nm dan 800 nm untuk mengevaluasi tingkat kematangan TBS kelapa sawit. *Komunikasi Fisika Indonesia*, **17**(3), 144.
17. Setiawan, A. W., Mengko, R., Putri, A. P. H., Danudirdjo, D., & Ananda, A. R. (2019). Classification of palm oil fresh fruit bunch using multiband optical sensors. *International Journal of Electrical and Computer Engineering*, **9**(4), 2386.
18. Azmi, M. H. I. M., Hashim, F. H., Huddin, A. B., & Sajab, M. S. (2022). Correlation study between the organic compounds and ripening stages of oil palm fruitlets based on the Raman spectra. *Sensors*, **22**(18).
19. Ali, M. M., Hashim, N., & Hamid, A. S. A. (2020). Combination of laser-light backscattering imaging and computer vision for rapid determination of oil palm fresh fruit bunches maturity. *Computers and Electronics in Agriculture*, **169**.



This article uses a license
[Creative Commons Attribution
 4.0 International License](https://creativecommons.org/licenses/by-nc/4.0/)